



Interpretation of remote sensing and aeromagnetic data to depict the structural framework of the transitional zone between the Igarra Schist belt and Anambra Basin, Nigeria

Naheem Banji Salawu^{1,2}

Received: 17 January 2022 / Accepted: 24 August 2022 / Published online: 8 September 2022

© The Author(s) under exclusive licence to Institute of Geophysics, Polish Academy of Sciences & Polish Academy of Sciences 2022

Abstract

High-resolution aeromagnetic and Landsat-8 data were utilized for the structural investigation of the Igarra Schist Belt located where the Precambrian crystalline basement is unconformably overlain by the late-Cretaceous Anambra Basin fill. Analysis of the Landsat-8 data exhibits major lineaments that trend in E–W, ENE–WSW, NNW–SSE and N–S directions. Results from the analysis of total field anomaly data using total gradient amplitude and tilt angle of the horizontal gradient also show these same lineament trends. The superimposition of Landsat-8 and aeromagnetic data-derived lineaments resulted in the mapping of the regional lineaments, which provide clues to structurally controlled gold mineralization in the Igarra Schist Belt region. Details mapped from the remote sensing data show surface contacts that correspond to the boundary between the Igarra Schist Belt and Anambra Basin mapped from aeromagnetic data. The source parameter imaging of the aeromagnetic data provides depth estimates of the magnetic basement of the Igarra Schist Belt and Anambra Basin, which varies from 50 to above 650 m. The integration of the remote sensing and aeromagnetic lineaments with the 3-D Euler deconvolution results reveals that the locations of cluster solutions alignment with lineaments are target areas for gold mineralization, which is correlative to gold occurrences in the region.

Keywords Aeromagnetic data · Gold · Anambra Basin · Remote sensing data · Igarra Schist Belt

Introduction

The occurrence and concentration of gold mineralization in the continental crust involve the combination of various geological processes, which include specific tectonic settings, unique structural framework and successive events of rock–fluid interaction (Groves et al. 2003; Pereira et al. 2019). Gold mineralization is established in supracrustal (schist) belts of western Nigeria mainly in primary veins, alluvial and eluvial placers (Garba 2003). The main factors controlling gold mineralization in the schist belts in Nigeria (Anka, Maru, Zuru, Zungeru–Birnin Gwari, Ilesa,

Karaukarau, Iseyin–Oyan, Kushaka and Egbe–Isanlu schist belts) are the geologic structures (Sanusi and Amigun 2020). Geological structures such as faults, fractures and shear zones, which are associated with gold mineralization, are regularly mapped using remote sensing and aeromagnetic data (Salmirinne and Turunen 2007). The enhancement of remote sensing and aeromagnetic data provides information on large-scale structural and geologic features such as surface lineaments, shallow geological structures, deep-seated faults, discontinuities and shear zones that may host gold mineralization (Ramadass et al. 2015; Eldosouky et al. 2022; Salawu et al. 2021a).

Remote sensing and aeromagnetic techniques have been extensively utilized to study schist belts in Nigeria, especially to identify lineaments that may host gold deposits (e.g., Andongma et al. 2020; Fagbohun et al. 2020; Sanusi and Amigun 2020; Salawu et al. 2021a). However, little is known about the association of gold mineralization with lineaments in the Igarra Schist Belt. Hence, there has been little progress in gold mineralization investigation in Igarra Schist Belt due to insufficient

Edited by Prof. Teresa Grabowska (ASSOCIATE EDITOR) / Prof. Gabriela Fernández Viejo (CO-EDITOR-IN-CHIEF).

✉ Naheem Banji Salawu
salawubanji@yahoo.com

¹ BS Geophysical and Consultancy Ltd., Ilorin, Nigeria

² Department of Geophysics, Federal University Oye-Ekiti, Oye-Ekiti, Nigeria

knowledge of the structural setting of bedrock gold mineralization in the study area. As such, the main objective of this study is to use remote sensing and aeromagnetic techniques to map and classify structural features associated with gold mineralization in Igarra Schist Belt. This study presents the results of the evaluation of regional structures in the Igarra Schist Belt, using a combination of aeromagnetic and remote sensing techniques to delineate lineaments associated with gold occurrences in the region. Several data processing techniques have been applied to the remote sensing and aeromagnetic data to determine lineaments that are associated with gold mineralization. The techniques used in this study include the Sobel directional filter, total gradient amplitude, tilt angle of the horizontal gradient, source parameter imaging and 3-D Euler deconvolution methods, each of which has significance in specific geological circumstances. The applied integrated techniques will provide insights into the structural setting of the region with high accuracy, which will decrease mineral exploration risk and highlight new gold mineralization opportunities that may lead to economic exploitation.

Geological setting of study area

The study region is located between 6° to 6° 30' E and 7° to 7° 30' N in southern Nigeria. It is underlain by crystalline basement, sedimentary cover rocks of the Nsukka Formation and post-Santonian Ajali Formation rocks of the Anambra Basin (Figs. 1 and 2). The Nigerian Basement Complex is cut by lineaments that form favourable pathways for mineralized fluids associated with the emplacement of quartz veins, pegmatite dykes, etc. Schist belts represent major features within the Nigeria Basement Complex (Garba 2003; Dada 2008). The schist belts of Nigeria, which consist of greenschist and amphibolite facies metavolcanic and metasedimentary rock units of Proterozoic age and Pan-African granitic plutons with widespread migmatization at approximately 620–580 Ma are well represented in Igarra, attesting to the extensive reworking during the multistage Pan-African Orogenic events (Dada 1998; Caxito et al. 2020). The tectonic evolution of the Nigerian schist belts in relation to the underlying crystalline basement was from the initial crustal extension, which was followed by continental rifting at the margin of the West African craton resulted in the development of graben-like structures in Western Nigeria that was followed by the deposition of rock units (mainly clastic sediments with minor volcanic rocks) of the schist belts (Ajibade et al. 1987). Closure of the ocean

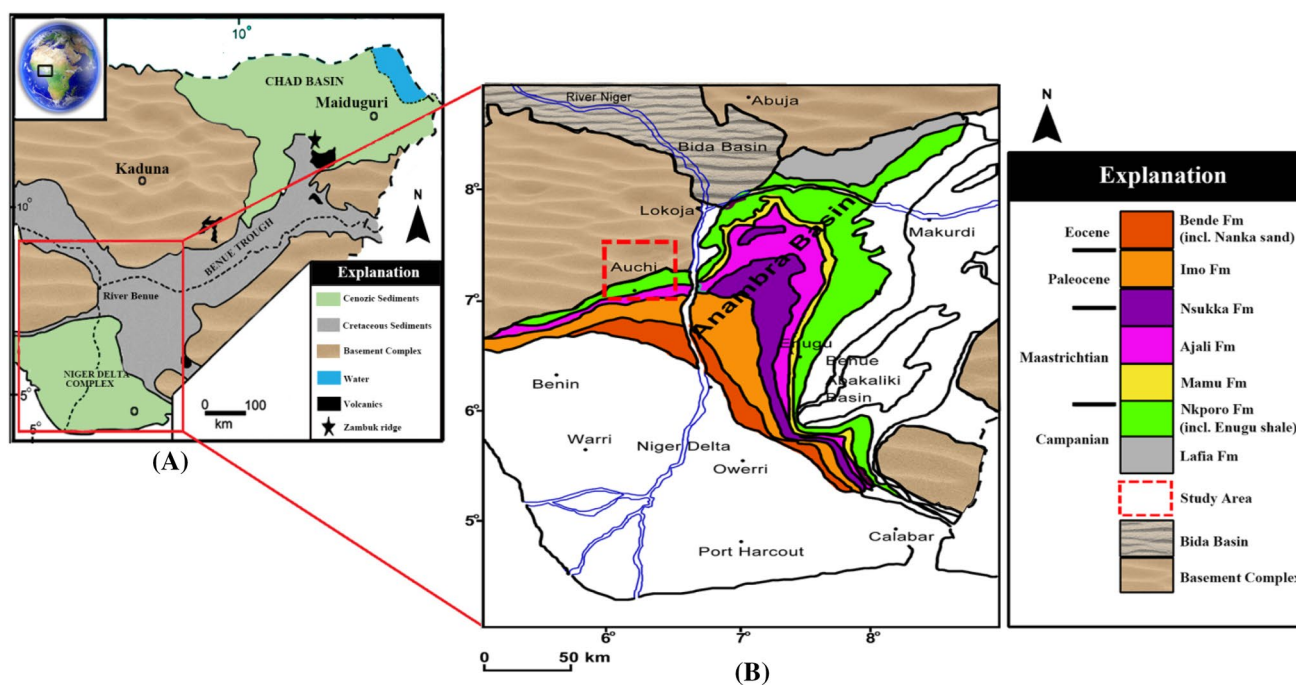


Fig. 1 a Simplified sectional geological map of Nigeria showing the basement terrain and sedimentary basins. b Generalized geological map of Anambra Basin with the studied region, specified with red dashed lines (modified after Adebayo et al. 2018)

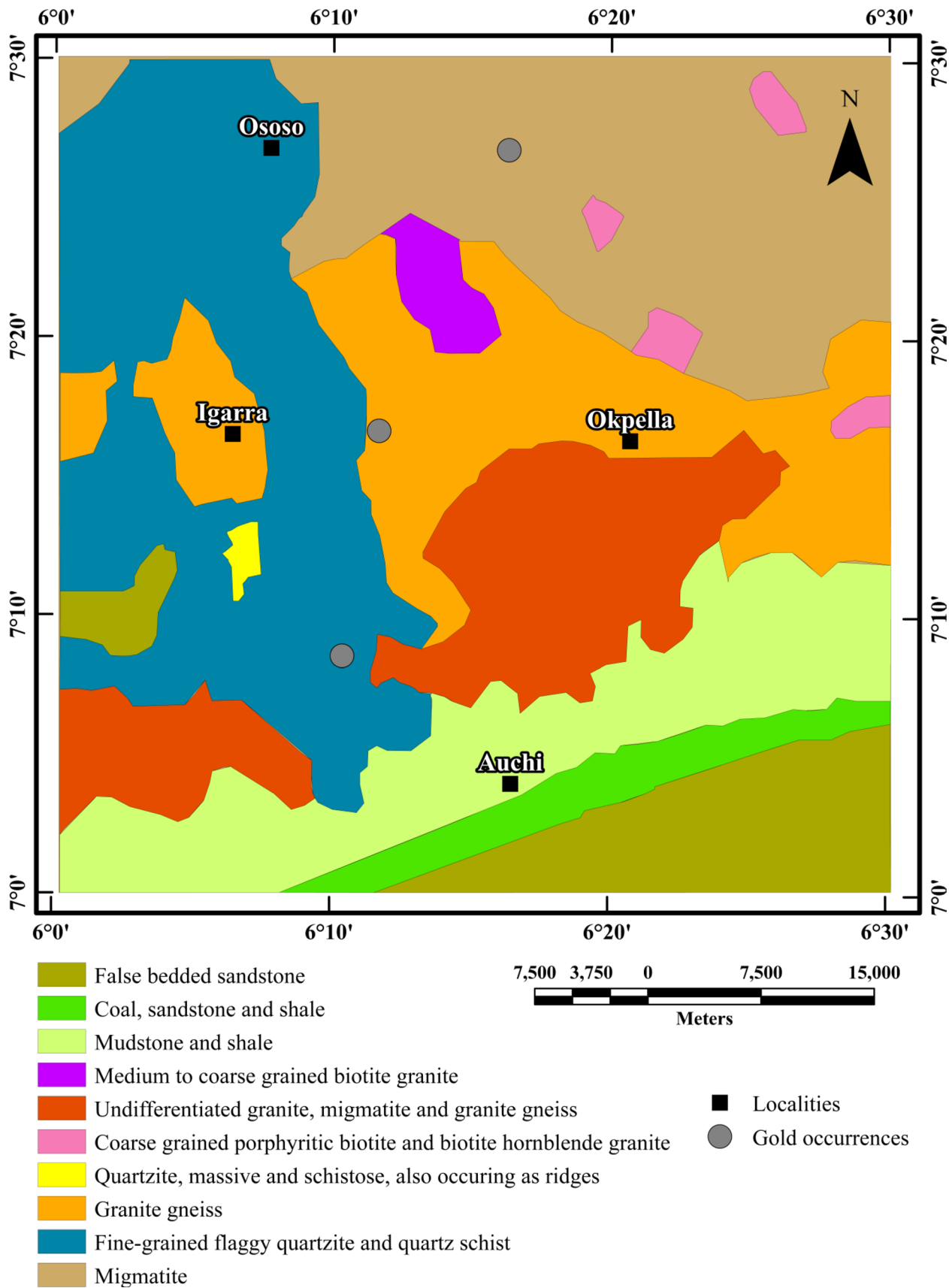


Fig. 2 Simplified geological map of the study area (NGSA 2011). Known gold occurrences are adopted from the mineral resources map of Nigeria (NGSA 2006)

at the margin of the West African craton at approximately 600 Ma and crustal thickening in the Dahomeyan resulted in the deformation of the sediments, the reactivation of preexisting rock units and the emplacement of the Pan-African granitoids (Ajibade et al. 1987).

The Igarra Schist Belt (Fig. 2), which forms a portion of the study area, represents the southern extension of the Egbe/Isanlu Schist Belt which hosts the Okolom gold field and various gold-quartz veins along local shear zones to the north (Garba 2003). The Igarra, Ososo and Okpella regions lie within the Igarra Schist Belt of the basement complex of Nigeria (Fig. 2). The Igarra Schist Belt is a N–S-trending synformal metasedimentary rock unit in-folded into the migmatite-gneiss. The Igarra Schist Belt comprises upper greenschist facies metapelites with interlayered quartzite, marble and metaconglomerate rock units (Ajibade et al. 1987). The metaconglomerate rocks comprise clasts, which were derived from the adjacent migmatite-gneiss complex (Odeyemi 1976). The Igarra Schist Belt consists of three main groups of rocks, which are: (1) migmatites, biotite and biotite-hornblende gneisses; (2) low-grade metasedimentary rocks (quartzites, polymict metaconglomerates, marbles, schists and calc-silicate gneisses); and (3) syn-to-late tectonic porphyritic, biotite- and biotite-hornblende granites, adamellites and granodiorites, gabbros and charnockites; unmetamorphosed dolerite, pegmatite, aplite and syenite dykes (Odeyemi 1988; Ogunyele et al. 2018).

Data and methodologies

Data

Remote sensing data

Remotely sensed data (path 189 and row 55) of Auchi and environs, which was downloaded from the United State Geological Survey (USGS) website, were acquired on December 31, 2017 by Landsat-8 OLI/TIRS satellite. The Landsat-8 data are free of cloud cover due to the period of its acquisition, which is the dry season; the visibilities of the Landsat-8 satellite sensors are highly improved during the dry season, which subsequently results in cloud-free data. The projection of the remotely sensed data is in UTM zone 32 N with projection units in meters using the WGS84 datum. Additionally, Shuttle Radar Topographic Mission digital elevation model data (resolution: 1-ARC) shown in Fig. 3 was downloaded from the USGS website and used in combination with the Landsat-8 data to assure adequate quality interpretations of morphological features.

Magnetic data

The total field anomaly (TFA) data (Fig. 4) of the Igarra Schist Belt and Anambra Basin is part of the aeromagnetic dataset of Nigeria, which was collected between 2003 and 2009, by Fugro Airborne Surveys on behalf of the Nigerian Geological Survey Agency. The purpose of the high-resolution magnetic survey was to foster the exploration of solid minerals within Nigeria. The magnetometer used for the magnetic survey was the 3 × Scintrex CS3 Cesium Vapour Magnetometer. The aeromagnetic measurements were taken at 80-m mean terrain clearance, with 500-m spacing flight lines in the NW–SE direction and 2-km tie line spacing. The aeromagnetic data were corrected for diurnal variation effects on site by the contractors. The geomagnetic field was removed from the diurnal-corrected aeromagnetic data using the International Geomagnetic Reference Field (IGRF) model.

Methods

Remote sensing method

The mapping of surface lineaments of the study area was achieved through the application of the directional filters of Sobel on the panchromatic band-8 of the Landsat-8 data using the Envi 4.8 software. The band-8 data was used since the qualities of deduced lineaments are dependent on the spatial resolution of the utilized data. The Sobel directional filters were applied to the panchromatic band-8 of the Landsat-8 data, using a convolution process by generating a window with a 3 × 3 pixel box of Sobel kernels. The windows of a 3 × 3 pixel box matrix for the Sobel directional filter operators in four trend directions is given in Salawu et al. 2021b. Four enhanced directional images were produced after the application of the Sobel directional filters, with enhanced lineament directions in the E–W, N–S, NW–SE, and NE–SW. These procedures allow the detection of surface lineaments in all probable directions. Hence, lineaments were automatically extracted from the four enhanced directional images. Lineaments were extracted automatically from the resulting Sobel directional images using the line module of the PCI Geomatica software. The Landsat-8 lineaments of the Igarra Schist Belt region were generated from the combination of extracted lineaments deduced from the four enhanced Sobel directional images. Also, auxiliary data indicating non-geologic features such as roads, lakes and rivers were superimposed on the extracted surface lineaments during the construction of the Landsat-8 lineaments of the region. This is to ensure that these non-geologic features are not mistakenly described as structurally related lineaments. Additionally, the rose diagram for Landsat-8 lineaments was produced using Rockworks software to disclose the trends of

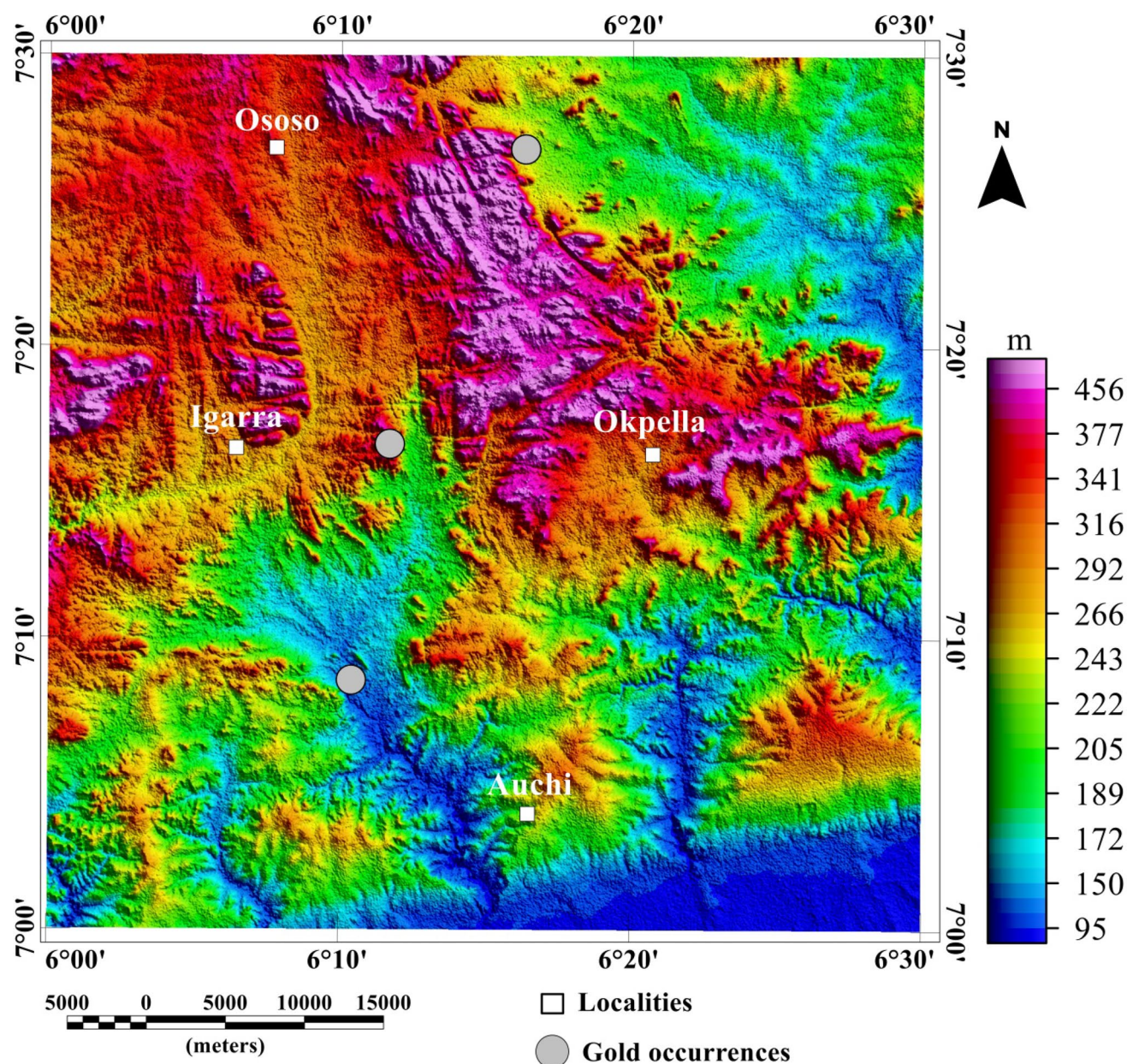


Fig. 3 Digital elevation model map of the Igarra Schist Belt and Anambra Basin

surface lineaments within the Igarra Schist Belt and Anambra Basin.

In addition, color combination technique was used for the analysis of the acquired Landsat-8 data, to reveal the morphological features of the study area. The human eyes are very sensitive and can differentiate the red, green and blue (RGB) colors. A color image is formed through the combination of three separate spectral bands of the Landsat-8 data and allocating the RGB colors to each band. A natural or true color image of the study area was achieved with a band combination of RGB = 432. The application of any color mixture excluding RGB = 432 is termed false color

composite (Alavi 2003). Hence, the true color composite map of the study area was deduced using the band combination of RGB = 432.

Magnetic method

In this study, the analysis of the diurnal and IGRF-corrected total field anomaly (TFA) data was carried out using various standard methods, namely the total gradient amplitude (TGA), tilt angle of the horizontal gradient (TAHG), source parameter imaging (SPI) and 3-D Euler deconvolution techniques. Each of the methods has numerous

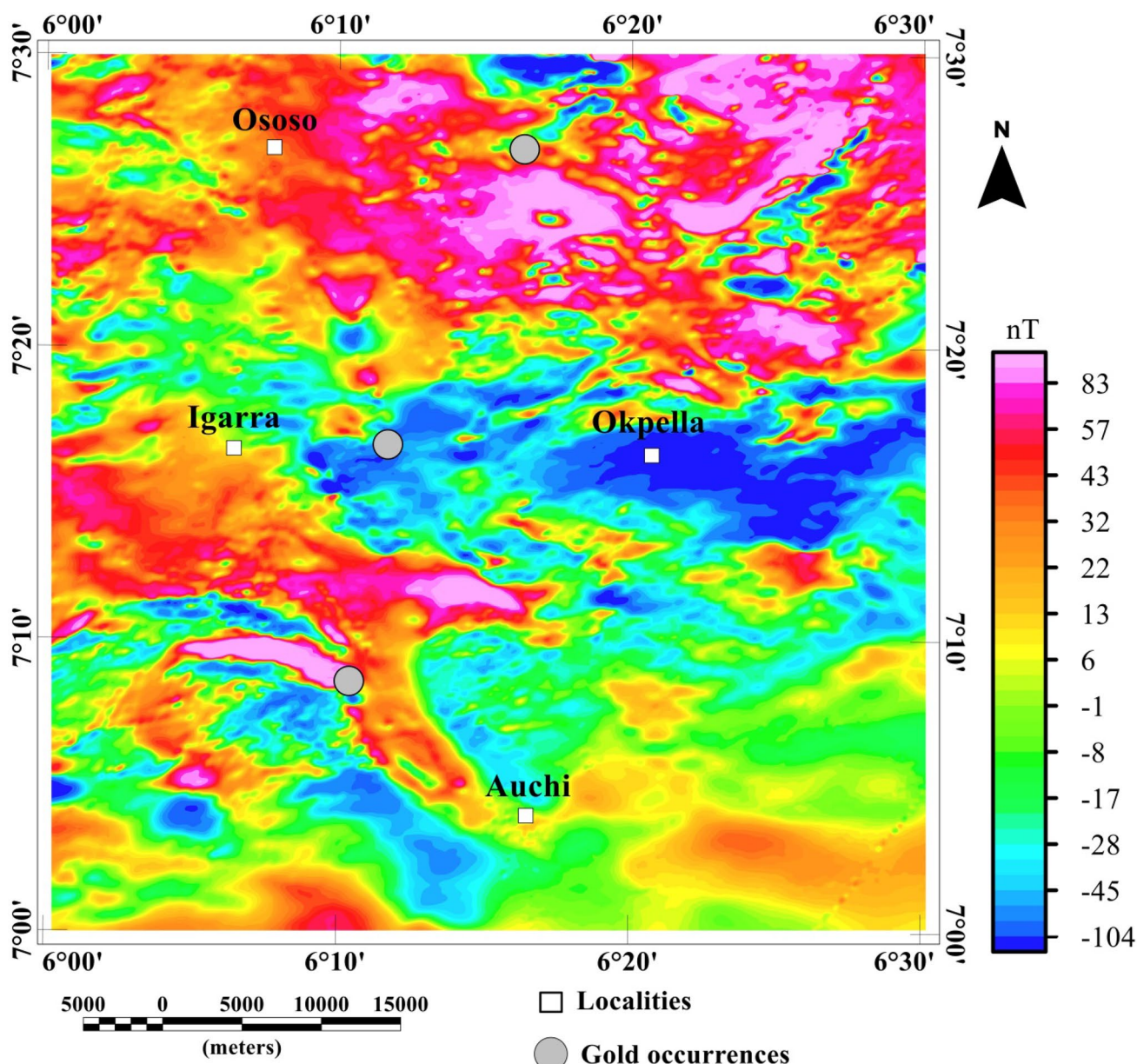


Fig. 4 The total field anomaly map of Igarra Schist Belt and Anambra Basin

significances in different geological settings. The utility of multiple methods to the same total field anomaly data improves the reliability of the results. The processing stages of the TFA data involve the following phases: **(a)** application of the reduction-to-pole (RTP) method on the TFA data to center anomalies above their respective magnetic sources. The parameters for the application of the RTP transformation are the inclination: -10.801° , declination: -2.484° and the total magnetic intensity value of 33,015 nT, which were selected at longitude: $6^\circ 15' E$ and latitude: $7^\circ 15' N$. In addition, amplitude correction inclination of 30° was used to achieve more stable responses of the RTP transformation,

which is unstable for low magnetic latitude regions (case of the studied area); **(b)** application of the directional cosine filter to the RTP data along the direction of magnetic declination (-2.484°) to reduce the artificial trends along the declination, which results from the RTP transformation; **(c)** mapping of shallow geological structures using the TGA of the TFA data; **(d)** application of the TAHG method to the corrected RTP-TFA data to map shallow to deep crustal structures; **(e)** extraction of peaks of the TGA and TAHG map to generate composite magnetic lineaments; **(f)** generation of the rose diagram of the study area from peaks of TFA-TGA and RTP-TAHG maps to establish trends

of magnetic lineaments; and **(g)** application of the SPI method to the TFA data to evaluation depth values of the magnetic basement; **(h)** application of 3-D Euler deconvolution technique on the TFA data for delineating locations and depth analysis of magnetic sources. The parameter used for the application of the 3-D Euler deconvolution method to the TFA data of the study area was a structural index of 1.0 for dyke sources, a window size of 2 km, and maximum depth tolerance of 6%. The summaries of the techniques used for the analysis of the TFA data of the study area is indicated in Table 1. In addition, an automatic lineament extraction procedure was applied to the TGA and TAHG maps to extract maxima of the TGA and TAHG signals to automatically detect lineaments within the study area. The regional aeromagnetic lineaments of the Igarra Schist Belt and Anambra Basin are established by integrating the results of the automatic extracted TGA and TAHG lineaments. The automatic lineament extraction procedure offers greater confidence in detecting lineaments and is also an effective way of establishing regional shallow- to deep-seated lineaments of the study area.

Results

Much insight into the distribution of anomalies resulting from magnetic geological sources within the studied region comes from the inspection of the produced reduced-to-pole total field anomaly map (Fig. 5). As discussed earlier, remotely sensed imagery can provide information about terrain-related features, which can be compared directly with geological structures derived from the analysis and interpretation of aeromagnetic anomaly data. Results from the depth analysis of the aeromagnetic anomaly data will aid the

interpretation of lineaments, with the estimates reflecting the depth values to the top of the magnetic sources in the region.

Reduced-to-pole magnetic map

Artificial trends in the direction of magnetic declination are observed in the reduced-to-pole (RTP) map in Fig. 5a, which are indicated with dashed black circles. However, the artificial trends are suppressed in the cosine-directional-corrected RTP map (Fig. 5b). The cosine-directional-corrected RTP total field anomaly map (Fig. 5b) shows both magnetic high and low anomalies of different wavelengths and amplitudes, with amplitude values varying from -66 to 90 nT. Magnetic high and low anomalies are more prominent and extend all over central and northern portions of the study area, passing areas such as Okpella, Igarra and Ososo with NE–SW and E–W trends. In the southern portion of the reduced-to-pole map, low magnetic anomalies are observed, which indicate weak magnetization within the Anambra Basin. This reveals that non-igneous sources are within the sedimentary layers producing weak and subtle magnetic anomalies within the southern part of the studied region.

Magnetic signatures related to lineaments

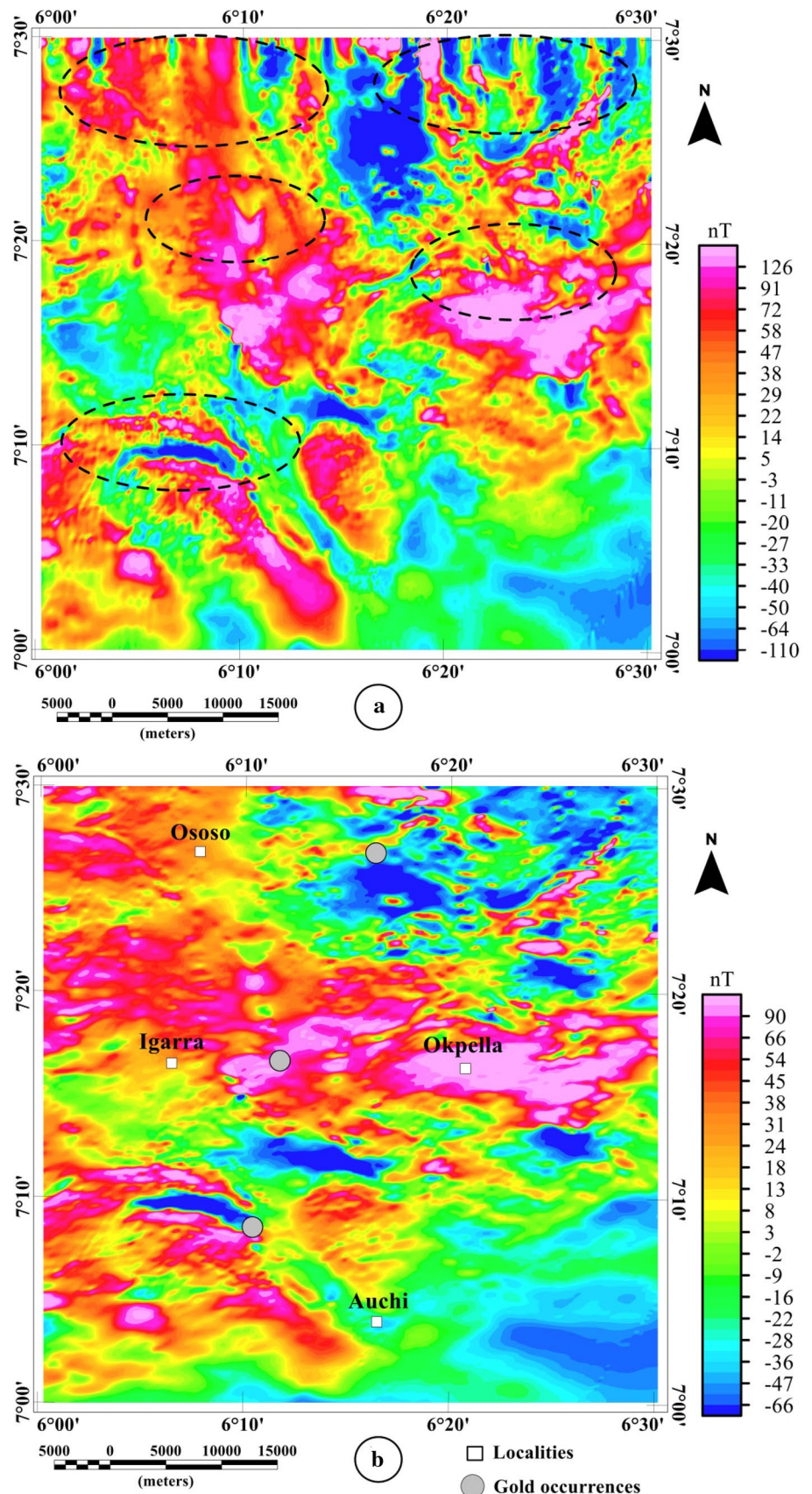
The TGA map (Fig. 6) reveals the structural pattern of the study area, which is marked by a predominance of E–W magnetic lineaments, but NW–SE and NE–SW alignments occur subordinately. Two main types of structural patterns are revealed on the TGA map: zones of strong (above 0.242 nT/m) and weak (<0.026 nT/m) (Fig. 6) gradients. The former is represented by linear structural patterns occurring in the central and northern parts of the study area (Igarra Schist Belt region), generally displaying a rough surface (high spatial frequency). The second type of structural pattern is located in the

Table 1 The techniques used for the analysis of the total field anomaly data of the study area

S/N	Methods	Equation	References
1	Total gradient amplitude	$TGA = \sqrt{\left(\frac{\partial F}{\partial x}\right)^2 + \left(\frac{\partial F}{\partial y}\right)^2 + \left(\frac{\partial F}{\partial z}\right)^2}$	Nabighian (1972; 1974); Nabighian (1984); (Roest et al. 1992); Salawu 2019a
2	Tilt angle of the horizontal gradient	$TAHG = \tan^{-1} \left(\frac{\frac{\partial THDR}{\partial z}}{\sqrt{\left(\frac{\partial THDR}{\partial x}\right)^2 + \left(\frac{\partial THDR}{\partial y}\right)^2}} \right)$	Ferreira et al. 2013
3	Source parameter imaging	$K = \frac{\frac{\partial^2 F}{\partial x \partial z} \frac{\partial F}{\partial x} + \frac{\partial^2 F}{\partial y \partial z} \frac{\partial F}{\partial y} + \frac{\partial^2 F}{\partial z^2} \frac{\partial F}{\partial z}}{\left(\frac{\partial F}{\partial x}\right)^2 + \left(\frac{\partial F}{\partial y}\right)^2 + \left(\frac{\partial F}{\partial z}\right)^2}$	Thurston & Smith 1997; Agustina 2019
4	3D Euler deconvolution	$(x - x_0) \frac{\partial F}{\partial x} + (y - y_0) \frac{\partial F}{\partial y} + (z - z_0) \frac{\partial F}{\partial z} = N(B - F)$	Thompson 1982; Reid et al. 1990; Reid et al. 2013; Salawu 2019b

F is given as the total field magnetic anomaly, B is the regional value of the total magnetic field and $THDR$ is the total horizontal gradient (Cordell and Grauch 1985; Phillips 1998; Phillips 2000; Phillips 2007; Salawu et al. 2019b)

Fig. 5 Reduced-to-pole total field anomaly maps of the studied region, derived after applying the reduction-to-pole filter on the aeromagnetic anomaly data of Igarra Schist Belt and environs. **a** Reduced-to-pole map showing the presence of artifacts (indicated with dashed black circles) arising due to the reduction-to-pole transformation. **b** Reduced-to-pole map corrected utilizing the cosine-directional filter



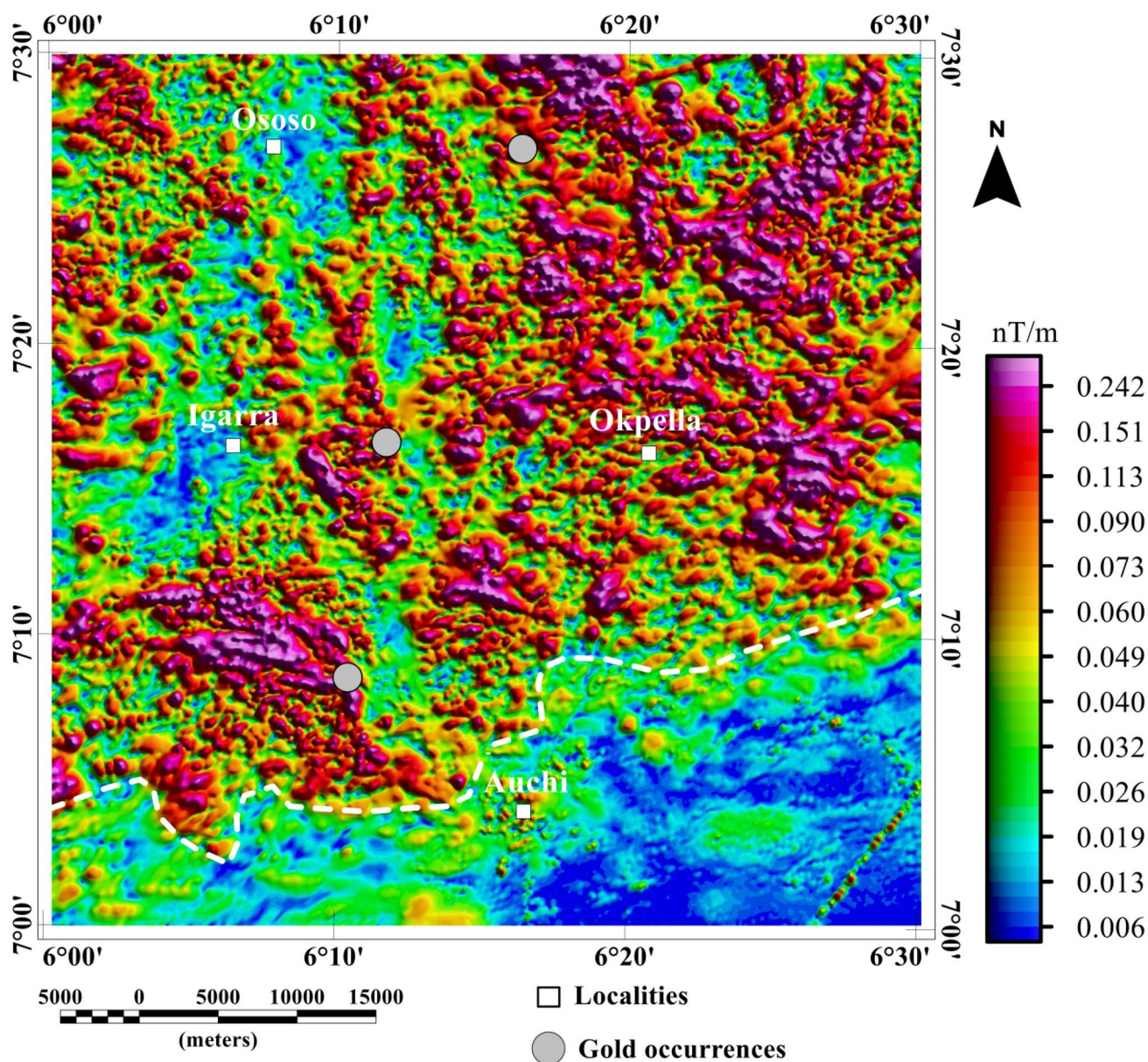


Fig. 6 Color-shaded total gradient amplitude (TGA) map of the aeromagnetic anomaly data, outlining magnetic contrasts within Igarra Schist Belt region. Maximum values of the TGA are observed mainly within the supracrustal terrain, while low TGA values are detected

within the Anambra Basin. The TGA peaks signify magnetic geological structures such as joints, faults and terrain boundaries. The interpreted boundary of the Igarra Schist Belt and Anambra Basin is indicated with white dashed lines on the TGA map

southern sector (Anambra Basin) and is characterized by flat magnetic relief, showing in the southeast, punctually, NE–SW-trending magnetic highs. The inferred boundary between the Igarra Schist Belt and Anambra Basin is marked by the contrast of minimum and maximum TGA values, indicated with dashed white lines on the TGA map. With the superimposition of the TGA structural features on the geological map of the study area (Fig. 7), it is easy to see lineament distributions within the Igarra Schist Belt region. The TGA lineaments are

poorly developed in the Anambra Basin in Fig. 7. The migmatite and schist rock units in Fig. 7 exhibit TGA lineaments mainly in the E–W and NE–SW directions. Lineaments with the E–W direction dominate the granite gneiss in the geological map (Fig. 7). The gold occurrences in the study area are associated with N–S- and E–W-trending lineaments in Fig. 7 and medium to high gradients (~ 0.060 – 0.242 nT/m) of the TGA in Fig. 6, which are concentrated in the Igarra Schist Belt.

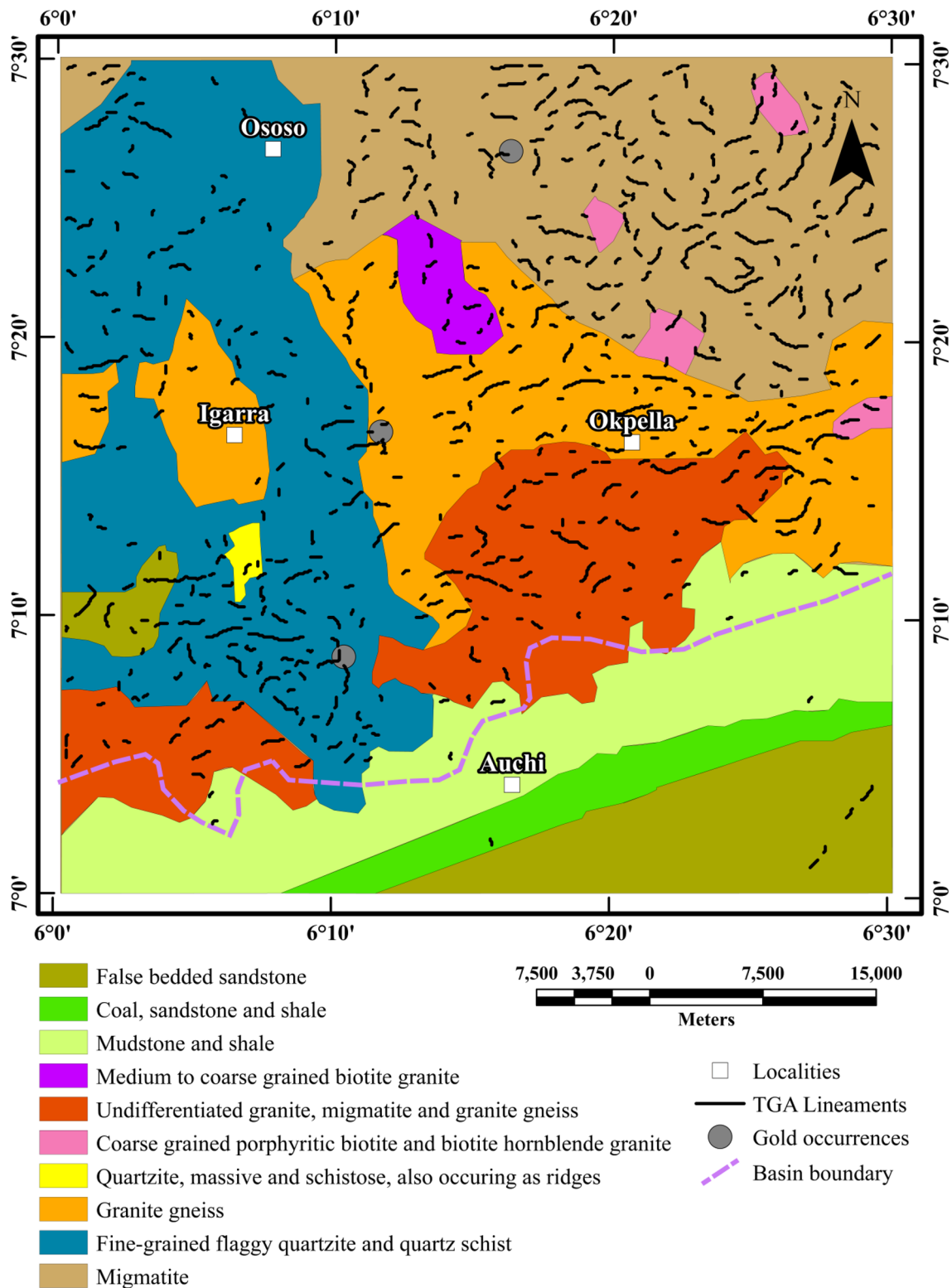


Fig. 7 The geological map of the study area with superimposed total gradient amplitude structural features. Note: The boundary of the Anambra Basin, which is indicated with dashed medium-lilac colored lines, is delineated from the total gradient amplitude map

However, the three gold occurrences in the region have in common the positioning in areas of high gradient (above 1.2 rad) in the tilt angle of the horizontal gradient (TAHG) map (Fig. 8). The TAHG map shows linear magnetic patterns related to shallow and deep magnetic lineaments that characterize the basement of the study area. The high values (above 1.2 rad) on the TAHG map reveal deep magnetic lineaments in the Anambra Basin, which are attenuated in the TGA map (Fig. 6). In addition, the TAHG map established deep-seated elongated lineaments in the Igarra Schist Belt, which were previously masked in the TGA map (Fig. 6). The true color composite (TCC) map (Fig. 9) clearly shows the suspected surface contacts between the Igarra Schist Belt and Anambra Basin, which appears on the TCC map as the abrupt transition of surface morphology in the southern portion of the studied region. The surface contacts are consistent with the superimposed sedimentary basin boundary (pink color dashed lines) deduced from the TGA map of the region. Hence, the gentle relief flat surface at the southern part of the TCC map, which provides a valid correlation with the TGA map, represents the Anambra Basin. The link was provided from the TGA, TAHG and TCC maps for subsurface structures and morphological features, and consequently, a valid lineament correlation is possible. The central and northern parts of the TCC map, which show distinct morphological patterns in comparison with the southern part of the map, represent the Igarra Schist Belt. The morphological patterns are commonly oriented E–W, possibly reflecting the network of lineaments in the Igarra Schist Belt.

Depth estimation of magnetic basement

The source parameter imaging (SPI) map (Fig. 10) shows the locations of different magnetic geological sources at different depths, with depth estimates varying from 50 to more than 650 m. It was observed in the southern part of the DEM map (Fig. 11a) that low elevation values below 95 m correlates with consistent and deeper depth values above 650 m within the Anambra Basin in Fig. 11b. The frequency of the depth estimates around the central and northern portions of the SPI map looks very high; spatially, it seems that a relatively short distance ranging from a low of ~ 50 m to high of ~ 250 m is prominent. The high frequency of depth values observed in the central and northern portion of the study area is interpreted as shallow magnetic basement within the basement terrain. The shallow magnetic basement correlates with high elevation (above 377 m) within the central and northern parts of the study area in the DEM

map (Fig. 11a). The magnetic basement depth values shown in the SPI map in most cases may correspond to the depth estimates of the crystalline basement of interest for mineral exploration. The SPI map shows the good correspondence of TGA lineaments over shallow depth values between 50 and 200 m in the central and northern regions of the study area.

Subsurface geological structures

The gray colored region in the southerly parts of the 3-D Euler deconvolution map (Fig. 12) corresponds to the Anambra Basin as revealed on the TGA map (Fig. 6). Buried dykes throughout the 3-D Euler deconvolution map produce clear cluster solutions with a shallow depth value less than 200 m, which extends to more than 600 m. The superimposed TGA and TAHG lineaments coincided with the 3-D Euler deconvolution solution trends in the locations for gold occurrences. Isolated TGA lineaments on the 3-D Euler deconvolution map (Fig. 12) reveal the location of shallow geological structures within the Igarra Schist Belt region. The shallow TGA lineaments are associated with gold mineralization within the study area. The TGA and TAHG lineaments that coincide together on the 3-D Euler deconvolution map indicate shallow-to-deep crustal-level structures. On the other hand, isolated TAHG lineaments on the 3-D Euler deconvolution map reveal deep-seated structures. Figure 12 reveals many deep-seated TAHG lineaments that align with TGA lineaments and superimpose 3-D Euler deconvolution solutions, thereby showing penetrative geological structures, which may have served as a channel for hydrothermal fluids migration, resulting in sulfides deposition and subsequently the formation of gold deposits.

Surface and subsurface structural appraisal

The aeromagnetic and Landsat-8 lineaments superimposed on the 3-D Euler deconvolution map correlate with Euler solutions in Fig. 13. Few common coincidences and convergence of both Landsat-8 and aeromagnetic lineaments on the 3-D Euler deconvolution map reveal that a limited number of surface lineaments reflects continuity at depth. Landsat-8 lineaments are interpreted as geologically related only where they have correspondence or align with TGA lineaments on the 3-D Euler deconvolution map. The main directions of the Landsat-8 lineaments as revealed by the rose diagram studied region (Fig. 13b) are E–W, NNW–SSE, N–S, and ENE–WSW. The main trends of the TGA lineaments

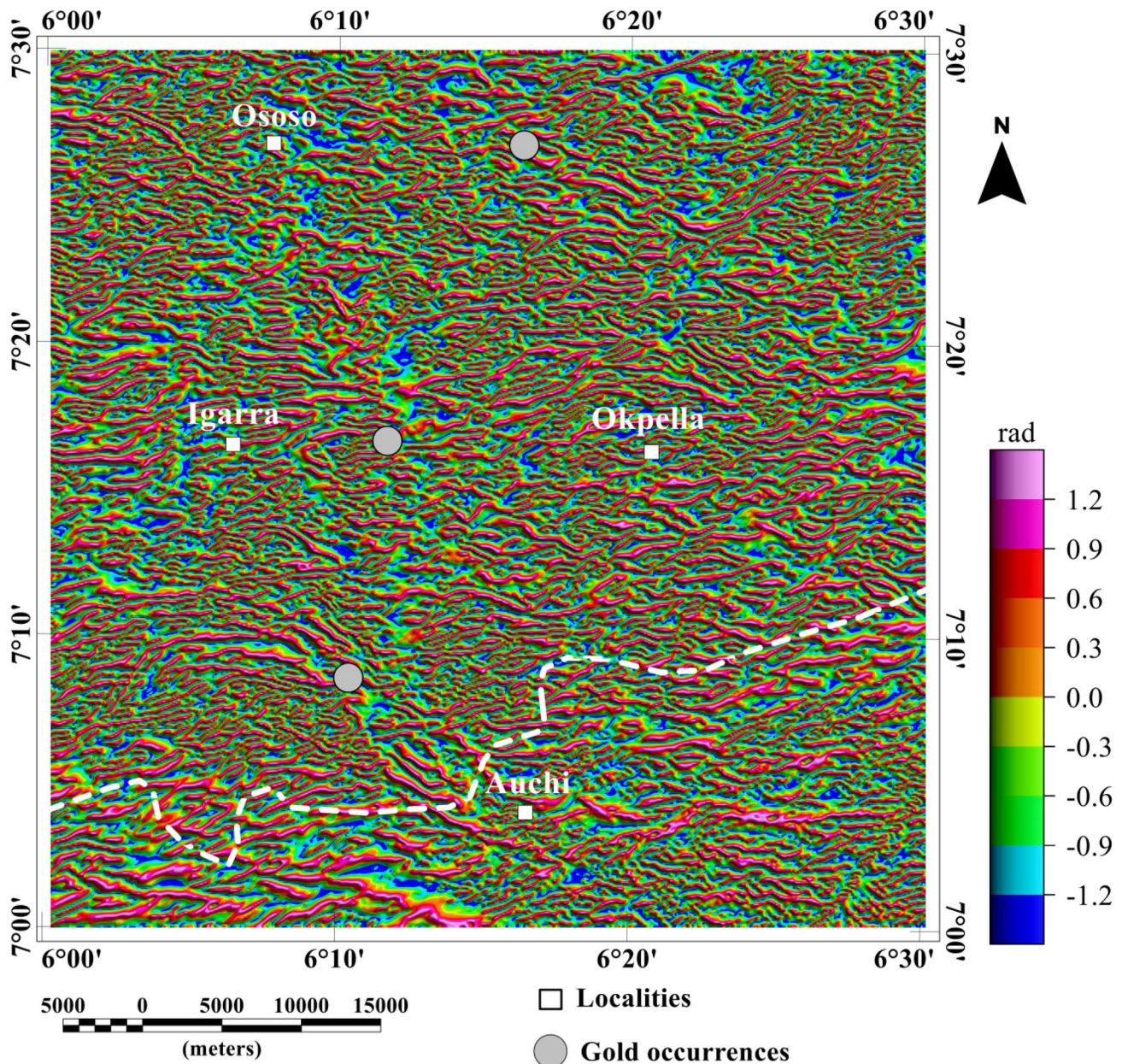


Fig. 8 Color-shaded tilt derivative map of the study area produced from the horizontal gradient magnitude of the cosine-directional-corrected reduced-to-pole aeromagnetic anomaly data. Maximum peaks of the tilt derivative map specify locations of shallow- to deep-seated

lineaments within the study area. The boundary of the Igarra Schist Belt and Anambra Basin indicated as white dashed lines on the tilt derivative map is delineated from the total gradient amplitude map

as shown in the rose diagram (Fig. 13c) are NW–SE, N–S, NE–SW and E–W, which complement and justify that the shallow structures in the region have surface manifestation.

Discussion

The advancement in magnetic data analysis over the last few decades has tended toward higher resolution of delineating shallow and deeper magnetic structural

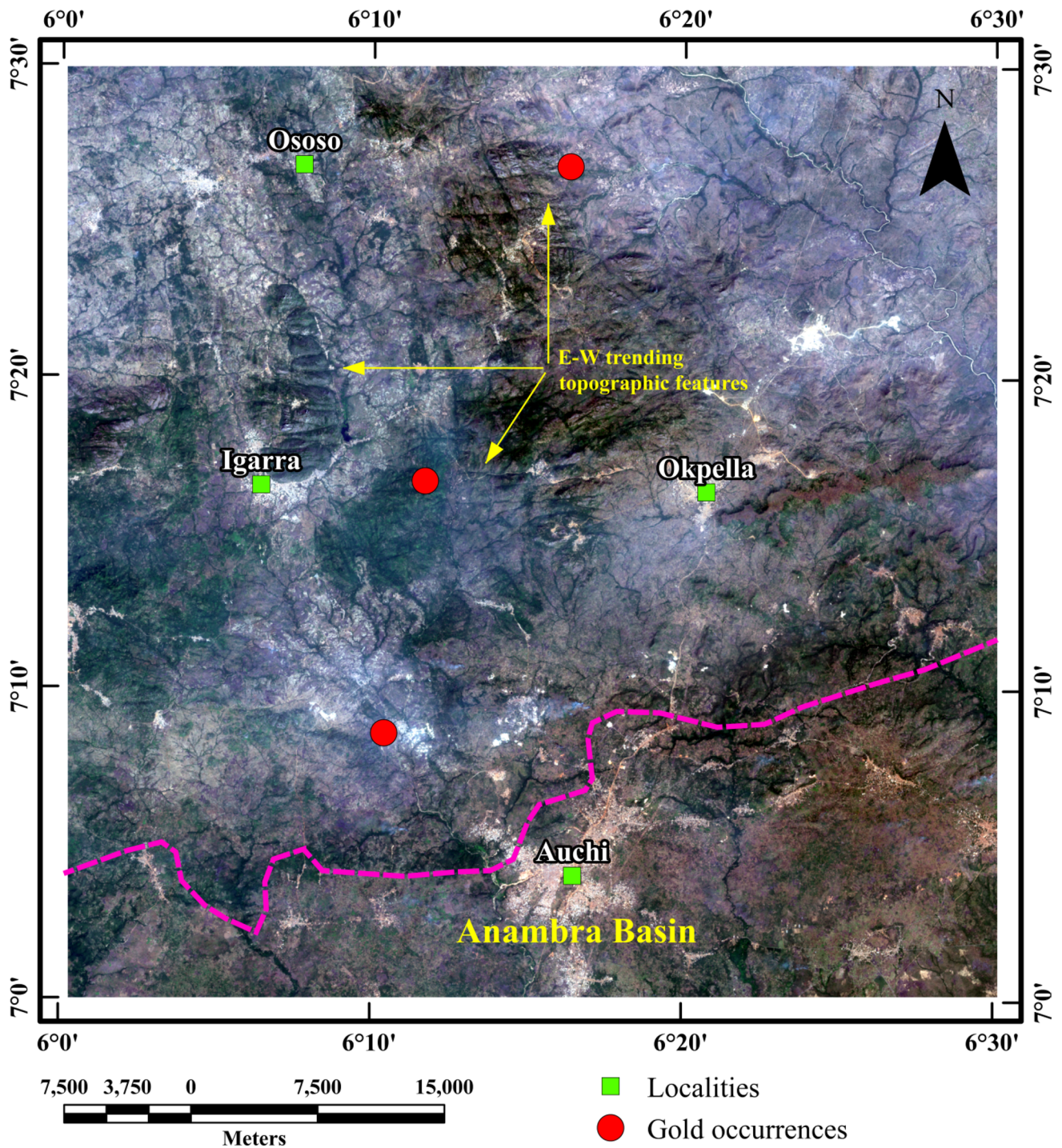


Fig. 9 True color composite (TCC) map deduced from the Landsat-8 bands (bands 432 in RGB) of the study area. The pink color dashed lines on the TCC map, which was deduced from the TGA map, indicate the boundary of the Igarra Schist Belt and Anambra Basin. The

transition in surface morphology in the southern part of the TCC map corresponds to the TGA sedimentary basin boundary, which is interpreted as the surface boundary between the Igarra Schist Belt and Anambra Basin

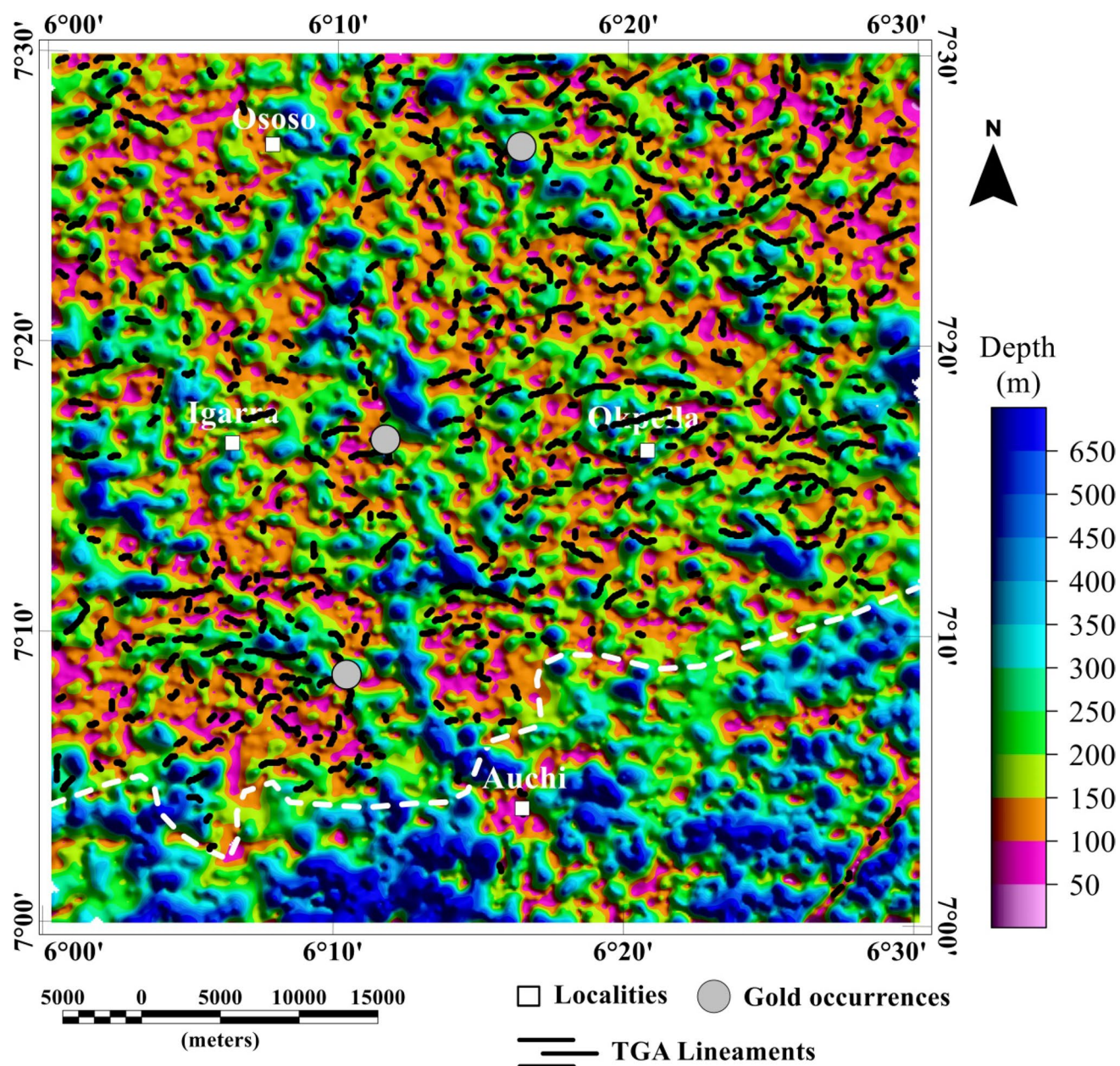


Fig. 10 Color-shaded source parameter imaging depth estimate map of Igarra Schist Belt and environs with superimposed boundary of the Anambra Basin (indicated with white dashed lines) and total gradient amplitude lineaments. Deeper depth estimated values are found

within the Anambra Basin (Auchi axis). However, shallower depth values are located within the Igarra Schist Belt regions such as Igarra, Ososo and Okpella areas

features such as intra-sedimentary and basement structures. Mapping of basement structures in particular can be very significant for understanding the general structural configuration of a region, even if mineral deposits are buried much deeper. Findings from this study reveal

that low magnetic anomalies are detected within the southern portion of the RTP magnetic anomaly map (Fig. 5b), which indicates weak magnetization within the Anambra Basin. This reveals the absence of igneous sources in the sedimentary formations of the Anambra Basin,

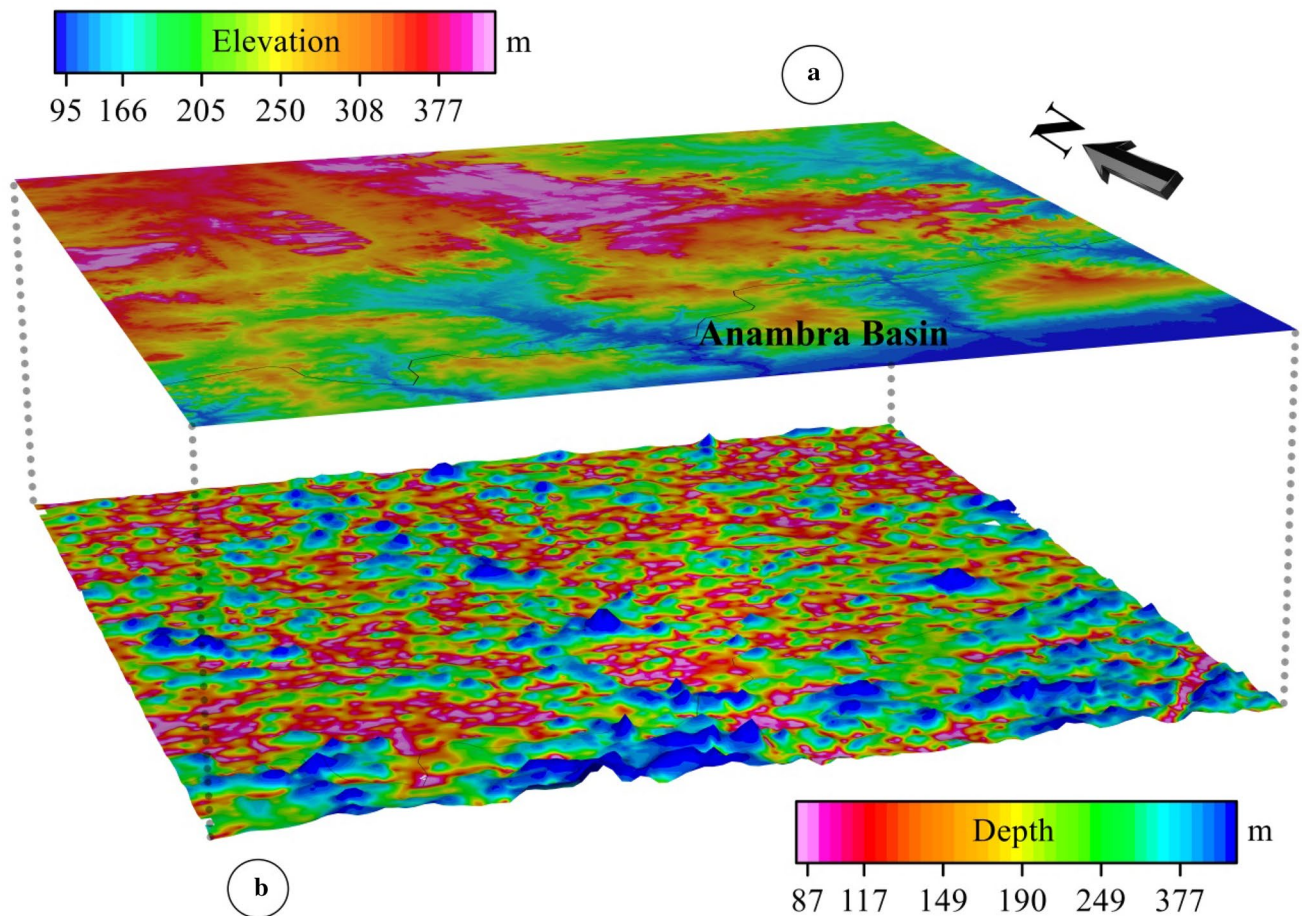


Fig. 11 Comparison of digital elevation model and source parameter imaging maps of the study area with superimposed boundary of the Anambra Basin, which is indicated with thin black lines. **a** Shuttle Radar Topographic Mission digital elevation model map of the study

area. **b** Depth to magnetic basement map, realized utilizing the source parameter imaging method showing magnetic source distributions within the studied region

which results in weak and subtle magnetic anomalies within the southern part of the RTP magnetic anomaly map. Peaks of the TGA were used to establish the shallow magnetic lineaments of the study area since the TGA losses greater coherence with depth, thereby providing shallow structures (Eldosouky et al. 2020). In comparison with the TGA, the results obtained from the TAHG map show deep crustal-level geological structures because the TAHG can delineate shallow- to deep-level lineaments (Ferreira et al. 2013). The main trends of the lineaments of the study area are the E–W, NW–SE, NNW–SSE, N–S, NE–SW and ENE–WSW directions. These trends from aeromagnetic and remote sensing data of the study area correspond to those previously documented as mapped during geological exercises in the study region (Ogunyele et al. 2018; Oden and Udinmwun 2014). With regard to the shallow aeromagnetic-structural framework of the region, lineaments that dominate the Igarra Schist Belt sequence

of the Basement Complex terrain are not deeply buried (see Figs. 7 and 12). The Igarra Schist Belt area (central and northerly parts of the study area) exhibits shallow structures trending in the E–W, NW–SE, N–S and NE–SW directions. Oden and Udinmwun (2014) reported two dominant trends of mineral veins through geological mapping in the study area, which are in the N–S and E–W directions. The N–S-trending mineral veins are thin, and the wider E–W-trending mineral veins are formed at depth (Oden and Udinmwun 2014). The dominant deep-seated trend pattern of the study area is in the E–W direction, which is now clearly evidenced on the TAHG and 3-D Euler deconvolution maps (Figs. 8 and 12, respectively) of the study region. Hence, as already stated by McCurry 1978, Salawu et al. 2021b; Salawu et al. 2021c and Salawu et al. 2020, the E–W structures are the oldest and can act as a pathway for the migration of hydrothermal fluids due to their deeper roots (see Figs. 8 and 12), which results in

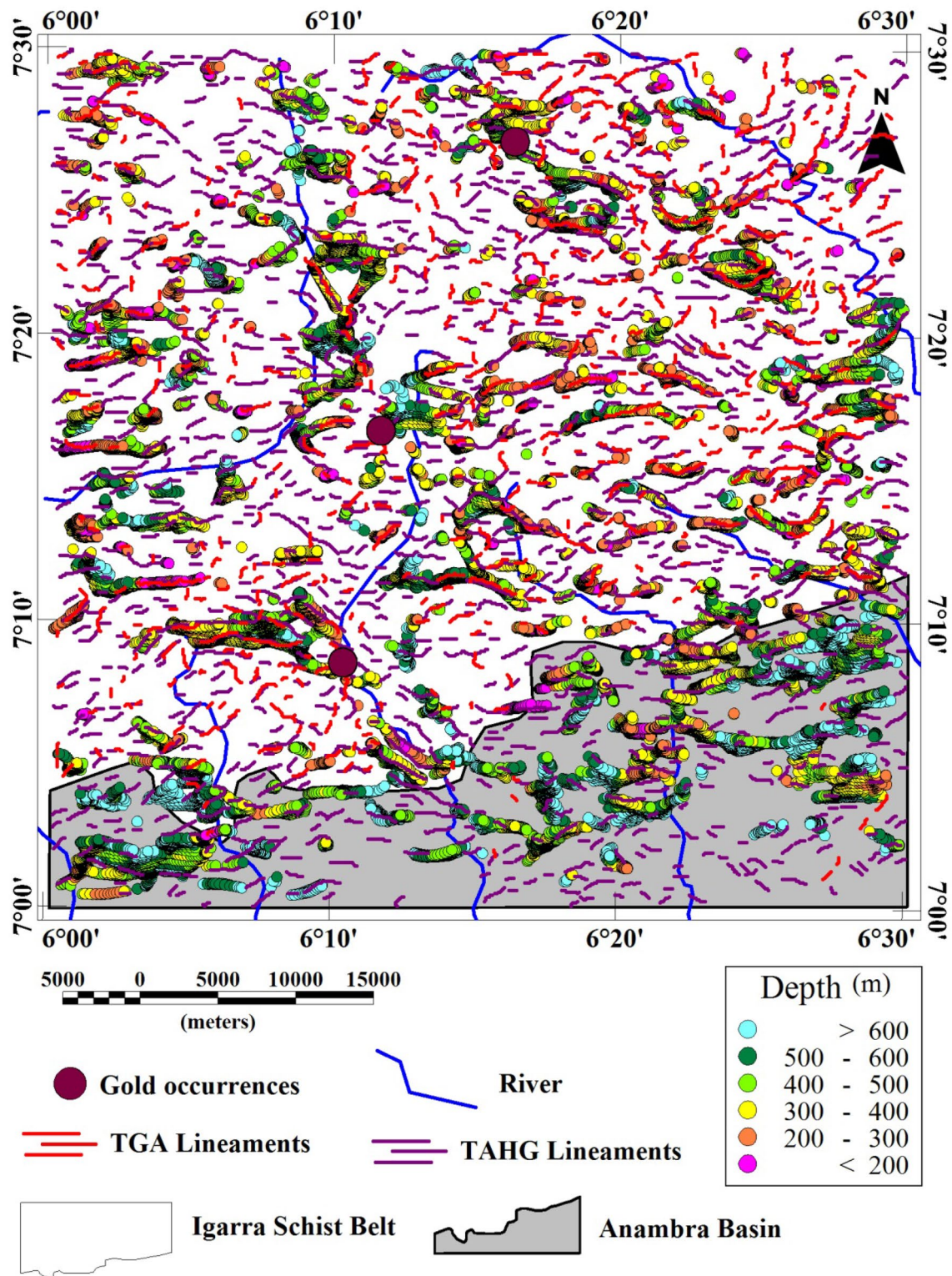


Fig. 12 The 3-D Euler deconvolution map of the Igarra Schist Belt and Anambra Basin with superimposed TGA and TAHG lineaments. TGA total gradient amplitude, TAHG tilt angle of the horizontal gradient

deposition of sulfides and subsequently formation of gold deposits.

The aeromagnetic data were very useful for mapping spatial locations of lineaments in the Igarra Schist Belt region at the margin of the Anambra Basin, where exploration for gold mineralization can be focused. Understanding whether the magnetic lineaments have surface manifestation is significant for assessing near or at surface exploration targets. However, there are common coincidences and convergence of both Landsat-8 and aeromagnetic lineaments on the 3-D Euler deconvolution map (Fig. 13a). An intuitive explanation for the convergence of Landsat-8 and aeromagnetic lineaments in the 3-D Euler deconvolution map (Fig. 13a) is that the converged lineaments are weak zones that can host gold mineralization. Moreover, the dominance of E–W topographic features on the TCC map (Fig. 9) strongly justifies the structural interpretation of the aeromagnetic data.

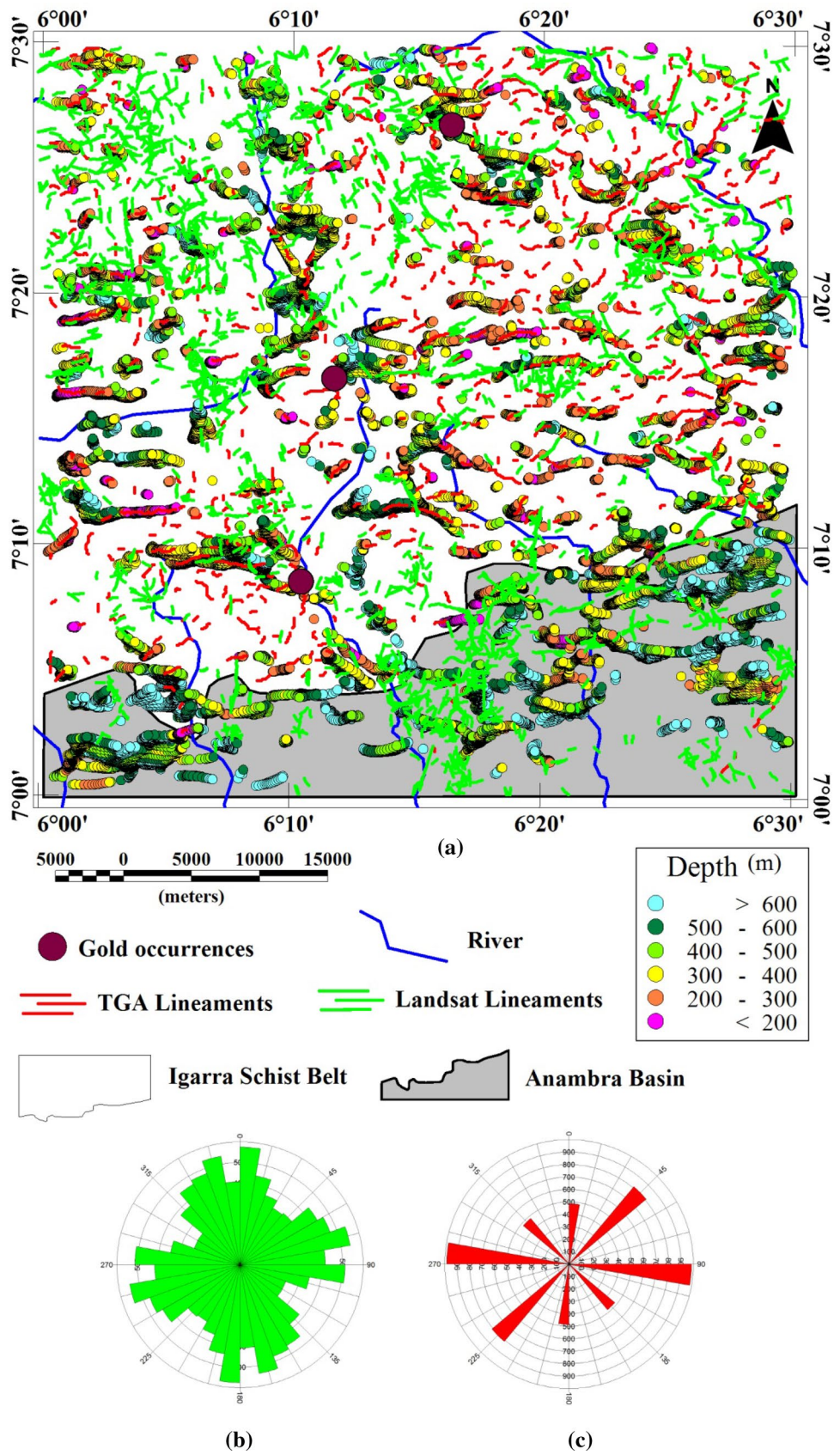
Low depth values to the top of magnetic sources in the studied region are associated with the Igarra Schist Belt, and deeper depth values are observed in than the Anambra Basin (Fig. 10). Again, the SPI depth variation allows the understanding of how shallow and deep the magnetic sources of the study area are. Findings obtained with the SPI map (Fig. 10) reveal that the magnetic basement in the central and northern parts of the study area with shallow depth values of 50 m is associated with TGA lineaments. The interpretation of the remote sensing and aeromagnetic maps provides evidence for the transitional zone between the Igarra Schist Belt and Anambra Basin, which properly discriminate between the basement and sedimentary basin structures. The cluster solution patterns in the 3-D Euler deconvolution maps (Figs. 12 and 13a) reveal the presence of intrusions in the form of dykes, which are usually associated with the Igarra Schist Belt (Odeyemi 1988; Ogunyele et al. 2018). The 3-D Euler deconvolution maps of the region show interconnecting Landsat-8 and aeromagnetic lineaments with intrusions (dykes) within the gold mineralized zone. The interconnected Landsat-8 and aeromagnetic lineaments can act as conduits for paleo-fluids produced by intrusions. The fluids would have remobilized the gold host basement rocks to concentrate the mineralization in the quartzitic lineaments. The alignment of 3-D Euler deconvolution solutions with aeromagnetic and Landsat-8 lineaments validates the importance of the remotely sensed and geophysical structural framework. The results of the geophysical structural framework reveal that lineaments are important in both surface and subsurface levels, especially in a tropical region such

as the study area where surface lineaments are masked by thick vegetation (Ajibade et al. 1987). Hence, the lineaments associated with the 3-D Euler deconvolution solutions in this study are likely related to mineralization and are associated with the gold occurrence locations in Figs. 12 and 13a. Therefore, the notable locations of the interlacement of remotely sensed and aeromagnetic lineaments with 3-D Euler deconvolution solutions in Figs. 12 and 13a are recommended areas where mineral exploration exercises can be carried out within the study area. This study reveals the significance of using remote sensing techniques for the mapping of surface lineaments that may be associated with structurally controlled mineralization as in the present study and are commonly obscured by thick vegetation cover. The present study also shows the importance of using aeromagnetic data to delineate the subsurface extension of surface lineaments, which provides good information on the percolation of mineralized fluids.

Conclusion

This research is focused on: (1) mapping of surface morphology within the Igarra Schist Belt region, using true-color composite image, (2) mapping of surface lineaments using Sobel directional filter and automatic lineament extraction procedures, and (3) mapping of aeromagnetic lineaments both at depth and extent using total gradient amplitude and tilt angle of the horizontal gradient methods. In addition, the source parameter imaging technique offers depth information of magnetic basement, which varies from 50 to 200 m. Hence, a composite lineament was produced from the combination of results realized from the analysis of aeromagnetic and Landsat-8 data. The superposition of aeromagnetic and Landsat-8 lineaments on the 3-D Euler deconvolution map of the study area offers fast identification of lineament distribution and its association with intrusions in the region. The major trends of lineaments in the region revealed by the total gradient amplitude and Landsat-8 rose diagrams are in the E–W, NW–SE, NNW–SSE, N–S, NE–SW and ENE–WSW directions. The 3-D Euler deconvolution map serves as a potential guide for detailed mineral exploration activities within the Igarra Schist Belt region. Finally, the outcome of this study shows that remote sensing and total field anomaly data are capable of mapping lineaments on a regional scale

Fig. 13 **a** The 3-D Euler deconvolution map of the Igarra Schist Belt and Anambra Basin with superimposed TGA and Landsat-8 lineaments. **b** Rose diagram generated from the Landsat-8 lineaments, revealing lineaments, which trend mostly in the E–W, NNW–SSE, N–S and ENE–WSW. **(c)** Rose diagram created from the TGA lineaments, which reveal lineaments that trend mainly in the E–W, NW–SE, N–S and NE–SW directions



that could serve as exploration guides and cost-saving tools.

Acknowledgements The author is very grateful to the management of BS Geophysical and Consultancy Ltd., for their support and the facilities made available during this research.

Data availability The Landsat 8 OLI/TIRS data used for this study are publicly accessible and can be downloaded from the US Geological Survey (USGS) website. However, the high-resolution aeromagnetic data are not publicly available, but can be acquired from the Nigeria Geological Survey Agency.

Declarations

Conflict of interest The author declare that there is no conflict of interest.

References

- Adebayo OF, Adegoke AK, Mustapha KA, Adeleye MA, Agbaji AO, Abidin NSZ (2018) Paleoenvironmental reconstruction and hydrocarbon potentials of upper cretaceous sediments in the Anambra Basin, southeastern Nigeria. *Int J Coal Geol* 192:56–72. <https://doi.org/10.1016/j.coal.2018.04.007>
- Agustina P, Mario EG, Guido MG, Andrés F, Patricia M (2019) Magnetic characterization of a retroarc extensional basin: The Loncopué Trough. *J South Am Earth Sci* 89:55–62
- Ajibade AC, Woakes M, Rahaman MA (1987) Proterozoic crustal development in the pan African regime of Nigeria. In: Kröner A (ed) Proterozoic lithospheric evolution. American Geophysical Union, Geodynamic Series, Vol 17. pp 259–271
- Alavi PS (2003) Application of remote sensing in geology (earth sciences), vol 1. University of Tehran, Tehran
- Andongma WT, Gajere JN, Amuda AK, Edmond RRD, Faisal M, Yusuf YD (2020) Mapping of hydrothermal alterations related to gold mineralization within parts of the Malumfashi Schist belt, North-Western Nigeria. *Egypt J Remote Sens Space Sci*. <https://doi.org/10.1016/j.ejrs.2020.11.001>
- Caxito F, Santos LCM, Ganade CE, Bendaoud A, Fettous E, Bouyo MH (2020) Toward an integrated model of geological evolution for NE Brazil–NW Africa: the Borborema Province and its connections to the Trans-Saharan (Benino–Nigerian and Tuareg shields) and Central African orogens. *Braz J Geol* 50(2):e20190122
- Cordell L, and Grauch VJS (1985) Mapping basement magnetization zones from aeromagnetic data in the San Juan Basin, New Mexico. In: Hinze WJ, ed., The utility of regional gravity and magnetic anomalies maps: SEG, 181–197
- Dada SS (1998) Crust-forming ages and Proterozoic crustal evolution in Nigeria: a reappraisal of current interpretations. *Precambrian Res* 87(1–2):65–74. [https://doi.org/10.1016/S0301-9268\(97\)00054-5](https://doi.org/10.1016/S0301-9268(97)00054-5)
- Dada SS (2008) Proterozoic evolution of the Nigeria–Borborema province. In: Pankhurst RJ, Trouw RAJ, de Brito Neves BB, de Wit MJ (eds) West Gondwana: pre-cenozoic correlations across the south Atlantic region. Geological Society, London, Special Publications 294: 121–136. <https://doi.org/10.1144/sp294.7>
- Eldosouky AM, Pham LT, Mohammed H, Pradhan B (2020) A comparative study of THG, AS, TA, Theta, TDX and LTHG techniques for improving source boundaries detection of magnetic data using synthetic models: a case study from G. Um Monqul, North Eastern Desert, Egypt. *J Afr Earth Sci* 170:103940. <https://doi.org/10.1016/j.jafrearsci.2020.103940>
- Eldosouky AM, Elkhateeb SO, Mahdy AM, Saad AA, Fnais MS, Abdelrahman K, Andrés P (2022) Structural analysis and basement topography of Gabal Shilman area, South Eastern Desert of Egypt, using aeromagnetic data. *J King Saud Univ Sci* 34:101764. <https://doi.org/10.1016/j.jksus.2021.101764>
- Fagbohun BJ, Omitogun AA, Bamisaiye OA, Ayoola FJ (2020) Remote detection and interpretation of structural style of the Zuru Schist belt, Northwest Nigeria. *Geocarto Int*. <https://doi.org/10.1080/10106049.2020.1753822>
- Ferreira FJF, Souza J, Bongiolo ABS, Castro LG (2013) Enhancement of the total horizontal gradient of magnetic anomalies using the tilt angle. *Geophysics* 78(3):33–41. <https://doi.org/10.1190/geo2011-0441.1>
- Garba I (2003) Geochemical characteristics of mesothermal gold mineralisation in the Pan African (600 ± 150 Ma) basement of Nigeria. *Appl Earth Sci* 112:319–325. <https://doi.org/10.1179/03717450325003143>
- Groves DI, Goldfarb RJ, Robert F, Hart CJR (2003) Gold deposits in metamorphic belts: overview of current understanding, outstanding problems, future research, and exploration significance. *Econ Geol* 98(1):1–29. <https://doi.org/10.2113/gsecongeo.98.1.1>
- McCurry P (1978) Geology of degree sheets 19 (Zuru), 20 (Chafe), and part of 19 (Katsina). Overseas Geological Mineral Resource, Nigeria, p 53
- Nabighian MN (1972) The analytic signal of two-dimensional magnetic bodies with polygonal cross-section: Its properties and use for automated anomaly interpretation. *Geophysics* 37:507–517
- Nabighian MN (1974) Additional comments on the analytic signal of two dimensional magnetic bodies with polygonal cross-section. *Geophysics* 39:85–92
- Nabighian MN (1984) Toward a three-dimensional automatic interpretation of potential field data via generalized Hilbert transforms: fundamental relations. *Geophysics* 49:780–786
- Nigerian Geological Survey Agency (NGSA) Mineral resources map of Nigeria (2006)
- Nigerian Geological Survey Agency (NGSA) (2011) Regional geology map of Lokoja and surroundings. Map prepared by NGSA. 31, Shetima Mangono Crescent Utako District, Garki, Abuja
- Oden MI, Udinmwun E (2014) Fracture Characterization, Mineral Vein Evolution and the Tectonic Pattern of Igarra Syn-Tectonic Granite, Southwestern Nigeria. *Br J Appl Sci Technol* 4(17):2417–2429
- Odeyemi IB (1976) Preliminary report on the field relationships of the basement complex rocks around Igarra, Midwest Nigeria. In: Kogbe CA (ed) Geology of Nigeria. Elizabethan Publ. Co., Lagos, pp 59–63
- Odeyemi IB (1988) Lithostratigraphy and Structural Relationships of the Upper Precambrian Metasediments in Igarra area, Southwestern Nigeria. In: Oluyide PO, Mbonu WC, Ogezi AEO, Egbuniwe IG, Ajibade AC and Umeji AC (eds.) Precambrian geology of Nigeria. Geological survey of Nigeria, Kaduna, 111–125
- Ogunyele AC, Obaje SO, Akingboye AS (2018) Lithostructural Relationships and Petrogenetic Affinities of the Basement Complex Rocks around Okpella. *Southwestern Nigeria. Earth Sci Malays* 2(1):29–36. <https://doi.org/10.26480/esmy.01.2018.29.36>
- Pereira LCL, Santos LCM, Carrino TA (2019) The role of airborne geophysics in the investigation of gold occurrences in the Itapetim Region, Borborema Province, Northeast Brazil *Braz J Geol* 49(3):e20190028. <https://doi.org/10.1590/2317-4889201920190028>

- Phillips JD, Hansen RO, Blakely RJ (2007) The use of curvature in potential-field interpretation. *Explor Geophys* 38:111–119
- Phillips JD (1998) Processing and interpretation of aeromagnetic data for the santa cruz basin - patahonia mountains area, South-Central Arizona. U.S. Geological survey Open-File Report, Arizona, 02–98
- Phillips JD (2000) Locating magnetic contacts: a comparison of the horizontal gradient, analytic signal, and local wavenumber methods. In: SEG technical program expanded abstracts, pp 402–405
- Ramadass G, Babu A, Preeti M (2015) Integration of aeromagnetic data and landsat imagery for structural analysis for discovery of kimberlites in parts of eastern Dharwar craton. *IOSR J Appl Geol Geophys* 3(4):1–15
- Reid AB, Allsop JM, Granser H, Millett AJ, Somerton IW (1990) Magnetic interpretation in three dimensions using Euler deconvolution. *Geophysics* 55:80–91
- Reid AB, Ebbing J, Webb SJ (2013) Avoidable Euler errors – the use and abuse of Euler deconvolution applied to potential fields. *Geophys Prospect*. <https://doi.org/10.1111/1365-2478.12119>
- Roest WR, Verhoef J, Pilkington M (1992) Magnetic interpretation using 3-D analytic signal. *Geophysics* 57(1):116–125. <https://doi.org/10.1190/1.1443174>
- Salawu NB, Olatunji S, Adebisi LS, Olasunkanmi NK, Dada SS (2019a) Edge detection and magnetic basement depth of Danko area, north-western Nigeria, from low-latitude aeromagnetic anomaly data. *SN Appl Sci* 1:1056. <https://doi.org/10.1007/s42452-019-1090-3>
- Salawu NB, Olatunji S, Orosun MM, Abdulraheem TY (2019b) Geophysical inversion of geologic structures of Oyo Metropolis, South-western Nigeria from airborne magnetic data. *Geomech Geophys Geo Energy Geo Resour* 5:143–157
- Salawu NB, Fatoba JO, Adebisi LS, Ajadi J, Saleh A, Dada SS (2020) Aeromagnetic and remote sensing evidence for structural framework of the middle Niger and Sokoto basins. *Nigeria Phys Earth Planet in*. <https://doi.org/10.1016/j.pepi.2020.106593>
- Salawu NB, Fatoba JO, Adebisi LS, Orosun MM, Dada SS (2021a) New insights on the Ife-Ilesha schist belt using integrated satellite, aeromagnetic and radiometric data. *Sci Rep* 11:15314. <https://doi.org/10.1038/s41598-021-94813-1>
- Salawu NB, Dada SS, Orosun MM, Adebisi LS, Fawale O (2021b) Influence of Pan-African tectonics on older Precambrian basement structural fabrics as revealed from the interpretation of aeromagnetic and remote sensing data of Ikole/Kabba region, southwestern Nigeria. *J Afr Earth Sci*. <https://doi.org/10.1016/j.jafrearsci.2021.104189>
- Salawu NB, Fatoba JO, Adebisi LS, Eluwole AB, Olasunkanmi NK, Orosun MM, Dada SS (2021c) Structural geometry of Ikogosi warm spring, southwestern Nigeria: evidence from aeromagnetic and remote sensing interpretation. *Geomech Geophys Geo Energy Geo Resour* 7:26. <https://doi.org/10.1007/s40948-021-00224-x>
- Salmirinne H, Turunen P (2007) Ground geophysical characteristics of gold targets in the central Lapland Greenstone Belt. *Geol Surv Finland Spec Pap* 44:209–223
- Sanusi SO, Amigun JO (2020) Structural and hydrothermal alteration mapping related to orogenic gold mineralization in part of Kushaka schist belt, North-central Nigeria, using airborne magnetic and gamma-ray spectrometry data. *SN Appl Sci* 2:1591. <https://doi.org/10.1007/s42452-020-03435-1>
- Thompson DT (1982) EULDPH-A new technique for making computer-assisted depth estimates from magnetic data. *Geophysics* 47:31–37
- Thurston JB, Smith RS (1997) Automatic conversion of magnetic data to depth, dip and susceptibility contrast using the SPI (TM) method. *Geophysics* 62:807–813

Springer Nature or its licensor holds exclusive rights to this article under a publishing agreement with the author(s) or other rightsholder(s); author self-archiving of the accepted manuscript version of this article is solely governed by the terms of such publishing agreement and applicable law.